

## Electron-irradiation defects in *n*-type GaAs

J. W. Farmer and D. C. Look

*Physics Department, University of Dayton, Dayton, Ohio 45469*

(Received 14 May 1979; revised manuscript received 2 October 1979)

We have studied the production and annealing of defects produced by 1-MeV electron irradiation of *n*-type GaAs. Two of these defects lie at 0.15 and 0.31 eV from the conduction band, respectively; in addition, there is at least one acceptor much closer to the valence band. The carrier-removal rate depends upon sample purity but is independent of the irradiation flux. The removal rate is also highly dependent upon the position of the the Fermi level, an effect which is considered in some detail. At about 200 °C, the defects recover in two stages, with the respective recovery rates given by  $\lambda_1 \approx 3 \times 10^8 \exp(-1.2/kT)$  and  $\lambda_2 \approx 1 \times 10^{12} \exp(-1.6/kT)$  where the energies are in eV;  $\lambda_2$  is somewhat dependent upon sample purity. In the highest-purity samples a reverse recovery phenomenon sometimes occurs, on about the same scale as  $\lambda_1$ . We present models for the production and recovery which are consistent with most of these results, as well as with other data found in the literature. It is suggested that the activation energies found in  $\lambda_1$  and  $\lambda_2$  may well be dissociation energies, rather than motional energies. Although the observed defects cannot be specifically identified, it appears that the level at 0.31 eV is a donor, and that at 0.15 eV is an acceptor; however, these conclusions are not firm.

### I. INTRODUCTION

Even though electron damage in GaAs has been investigated for nearly two decades, there still is a lack of consensus on its two most fundamental aspects: defect production rate and defect annealing. The defect production rate is generally determined from the free-carrier removal rate ( $dn/d\phi$ ). The wide variation in the values of  $dn/d\phi$  reported in the literature leaves open the question of whether the defect production rate itself varies or whether the proportionality between defect production rate and  $dn/d\phi$  varies. In the area of defect annealing, no detailed study of defect annealing kinetics has been made since Aukerman's original study.<sup>1</sup> Since high-purity GaAs epitaxial layers are now available, a more detailed investigation of annealing in this material is now possible.

This paper reports the investigation of defect production in 1-MeV electron-irradiated *n*-type GaAs. In particular, the dependence of the defect production rate on fluence and the relationship between defect production rate and free-carrier removal rate are addressed. In addition, the annealing kinetics of the 200 °C annealing stage (evidently associated with the Ga sublattice<sup>2</sup>) are studied in doped and high-purity GaAs.

### II. PROCEDURE

Most of the samples used in this work were high-purity, vapor-phase epitaxial (VPE) layers grown in our laboratory. In addition, several other VPE, liquid-phase epitaxial (LPE), and bulk GaAs samples

were obtained from a variety of manufacturers. All epitaxial layers were grown on Cr-doped GaAs substrates. Electrical measurements were carried out using a standard, five-contact, Hall-bar configuration<sup>3</sup> with indium contacts. The 1-MeV electron irradiations were made at room temperature.

When electrical measurements are used to monitor defect production in semiconductors, it is generally assumed that the free-carrier removal rate ( $dn/d\phi$ ) is proportional to the defect introduction rate. It can be shown that this assumption is valid as long as the Fermi level is not significantly changed by the introduction of the defects. A general rule of thumb has been that  $dn/d\phi$  is proportional to the defect introduction rate if the initial free-carrier concentration is changed by less than 10%. This convention has been observed in this work.

### III. RESULTS

#### A. Production

Figure 1 shows the free-carrier removal ( $\Delta n$ ) as a function of fluence for a large number of GaAs samples surveyed in this work. As stated earlier, the samples (bulk, VPE and LPE) were obtained from several sources and contained different dopants. Two features of these data are of particular interest. First, almost without exception defect production is less than linear with fluence. (For the few samples which did exhibit linear production, it was found that subsequent annealing and then further irradiation gave not only sublinear production but also a *higher* production rate.) The average of all the data in Fig. 1 yields

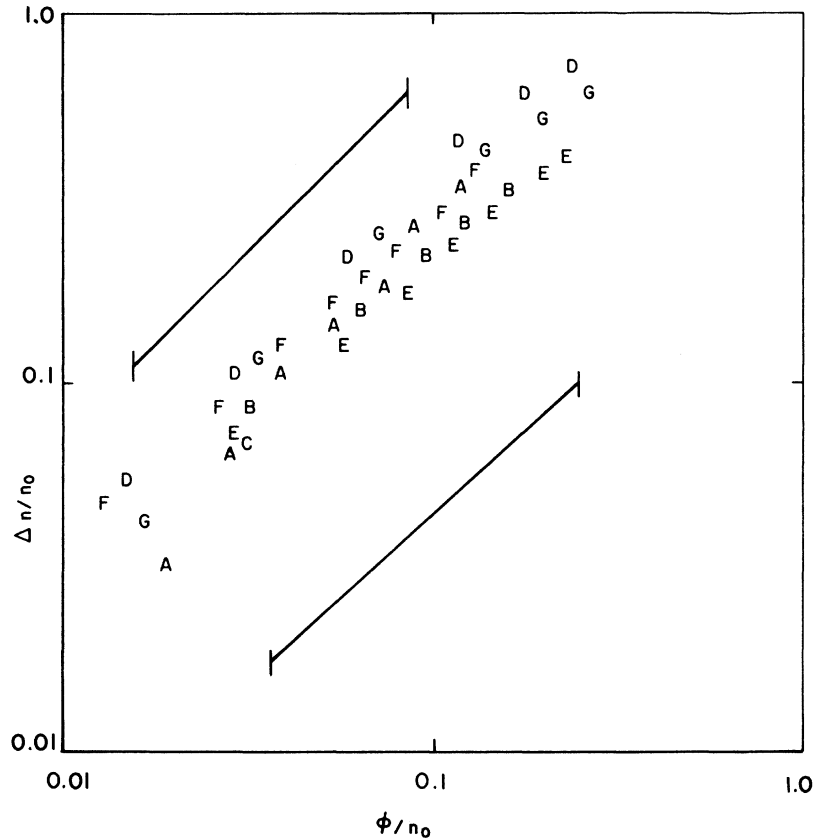


FIG. 1. Free-carrier removal vs fluence for a portion of the samples surveyed in this work. The solid lines represent the range of values reported in the literature.

$\Delta n \propto \phi^{0.86}$ . While the data shown in Fig. 1 pertain to doped samples, the production is also found to be sublinear in high-purity epitaxial layers. The second point of interest derived from Fig. 1 is the scatter in the free-carrier removal rate ( $dn/d\phi$ ). Although there are significant variations in our  $dn/d\phi$ , still they are quite small compared to the range of values reported in the literature (represented by the solid lines). Also, it appears that the free-carrier removal rate is uncorrelated with dopant species, manufacturer, or method of growth. (Kol'chenko and Lomako<sup>4</sup> also report no dependence on dopant species.)

We must consider the possibility that the variation in  $dn/d\phi$  may be due to a flux dependence, such as has been reported for ion implantation.<sup>5,6</sup> Electron flux is rarely reported and thus a determination of a dependence of  $dn/d\phi$  on flux from the data in the literature is not feasible. To investigate this problem we have measured the free-carrier removal rate as a function of fluence, for two widely different fluxes, and the results are shown in Fig. 2. Most other samples showed similar behavior. One sample appeared to have a small flux dependence (i.e., higher flux, larger free-carrier removal rate); however, even in

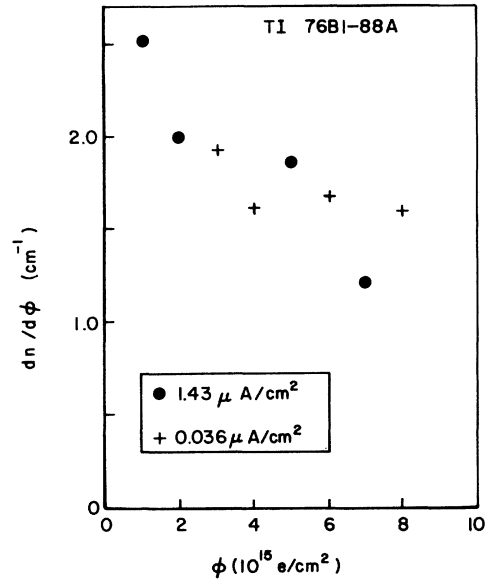


FIG. 2. Free-carrier removal rate vs fluence for two widely different fluxes.

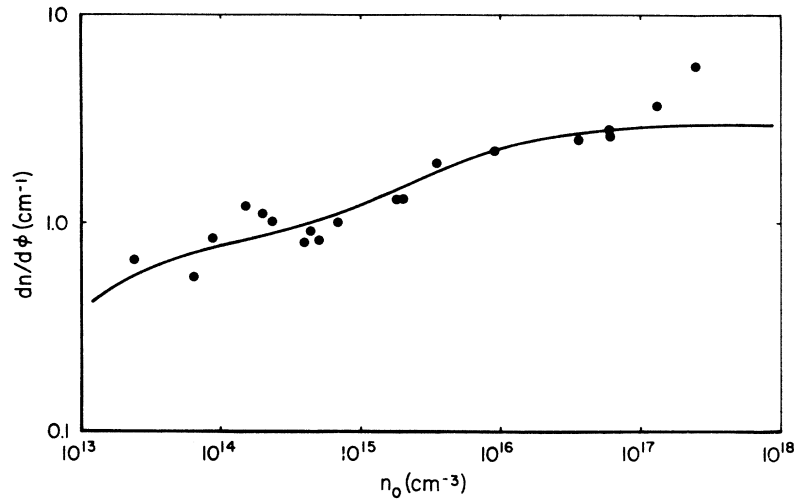


FIG. 3. Free-carrier removal rate vs  $n_0$ . The curved line is the calculated removal rate for a constant (i.e., independent of  $n_0$ ) production rate of two defects. The defects are assumed to be acceptors at 0.16 and 0.31 eV (with respect to the C.B.) with production rates of 2.2 and  $0.8 \text{ cm}^{-1}$ , respectively.

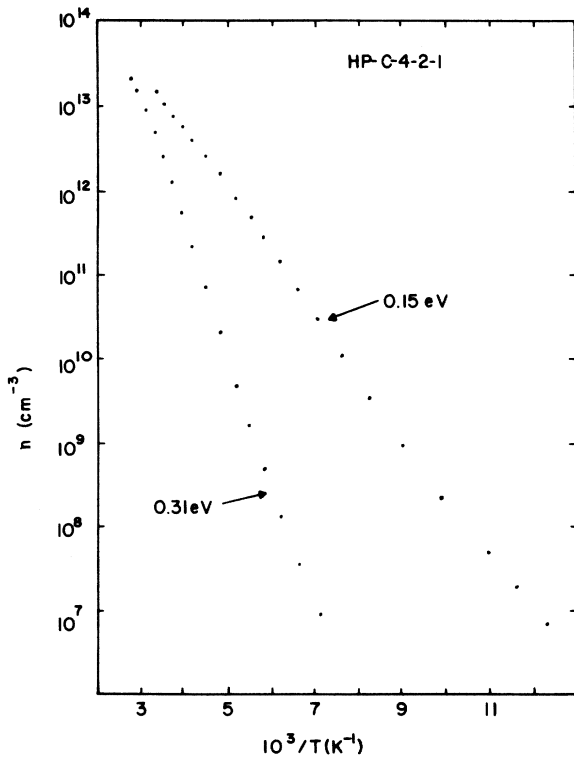


FIG. 4. Free-carrier concentration vs inverse temperature for two fluences. Defect levels of 0.15 and 0.31 eV are observed following irradiation fluences of  $1.0$  and  $2.0 \times 10^{14} \text{ e/cm}^2$ , respectively. The pre-irradiation free-carrier concentration was  $2.0 \times 10^{14} \text{ e/cm}^3$ .

this case the result was not statistically significant because of large scatter in the data.

While no clear correlations between  $dn/d\phi$  and material parameters were obtained for doped samples, a strong correlation between  $dn/d\phi$  and initial carrier concentration  $n_0$ , can be found in undoped samples. Figure 3 shows  $dn/d\phi$  as a function of  $n_0$ . The solid line is obtained from a calculation based on a model which will be discussed later.

In Fig. 4 we show Arrhenius plots of data from one of our samples. The calculated energy levels of 0.15 and 0.31 eV, respectively, agree quite well with those of other samples studied here and in other laboratories. It should be noted that a third level has also been reported and a review by Lang<sup>7</sup> lists the "best" values for the three levels as,  $E1 = 0.13 \text{ eV}$ ,  $E2 = 0.20 \text{ eV}$ , and  $E3 = 0.31 \text{ eV}$ . It is not clear whether our 0.15-eV level is, in fact,  $E1$  or an unresolved combination of  $E1$  and  $E2$ .

### B. Annealing

Figure 5 shows the data for a  $200^\circ\text{C}$  isothermal anneal of a doped sample. The Hall-effect data were collected *in situ* at  $200^\circ\text{C}$ . The data can be resolved into two substages which will be referred to as  $\lambda_1$  and  $\lambda_2$ , in Aukerman's notation.<sup>1</sup> Each substage is first-order (see insert), i.e., the recovery process can be described by

$$\Delta n(t) = \Delta n_1 \exp(-\lambda_1 t) + \Delta n_2 \exp(-\lambda_2 t) \quad (1)$$

where  $t$  is time,  $\Delta n(t) \equiv n(t) - n(\infty)$  ( $n$  is the free

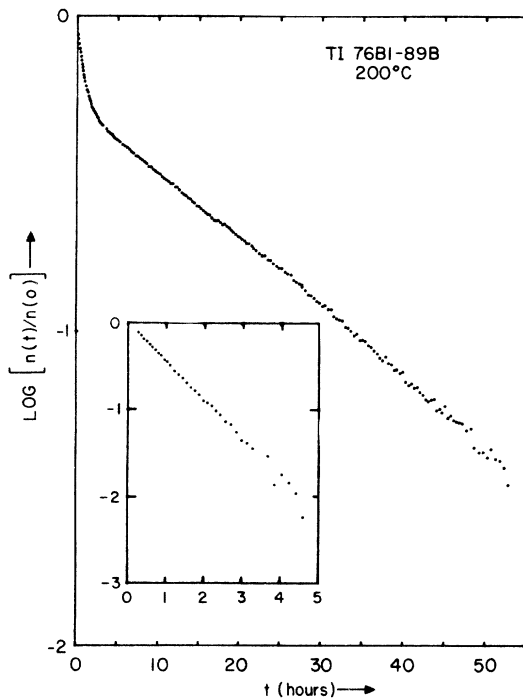


FIG. 5. Isothermal anneal at 200°C. The insert is obtained by subtracting the linear portion of the curve (extrapolated back to zero time) from the rest of the data. The axis scales in the insert are the same as in the main figure.

carrier concentration),  $\Delta n_1$  and  $\Delta n_2$  are the portions of free carriers initially removed by the defect (or defects) associated with each respective annealing substage, and  $\lambda_1$  and  $\lambda_2$  are the annealing rates of the respective substages. The temperature dependences of the annealing rates were found to be

$$\lambda_1 \approx 3 \times 10^8 \exp(-1.2/kT) \text{ and } \lambda_2 \approx 1 \times 10^{12} \times \exp(-1.6/kT).$$

Annealing was also studied in undoped samples. However, interpretation of the results is not as straightforward as in the case of doped samples. In high-purity samples the Fermi level may be below some of the defects and the occupation of a substantial fraction of the defects is very strongly dependent on temperature. The annealing rate for the  $\lambda_2$  defect substage was measured and the results are shown in Fig. 6. Data from our study indicate that  $\lambda_2$  is approximately constant at moderate to high doping levels and is decreasing as the purity increases for the undoped samples. Additional data from the literature are included for comparison. The totality of points can be roughly fitted by a line of slope  $\frac{1}{3}$ , i.e.,  $\lambda_2 \propto n_0^{1/3}$ ; this relationship will be discussed in more detail later.

#### IV. DISCUSSION

##### A. Production

The form of the defect production (linear or non-linear) can often help determine the kinds of defects and their production mechanisms. In the majority of the samples surveyed in this work it is clear that the defect production is not linear with fluence. Defect production in GaAs has often been reported to be linear; however, a careful review of the reported data<sup>1,8-11</sup> shows that in fact *most* of the data are actually only *nearly* linear (in agreement with the findings reported here).

In general, defect production will be linear with fluence if the defects do not interact with each other

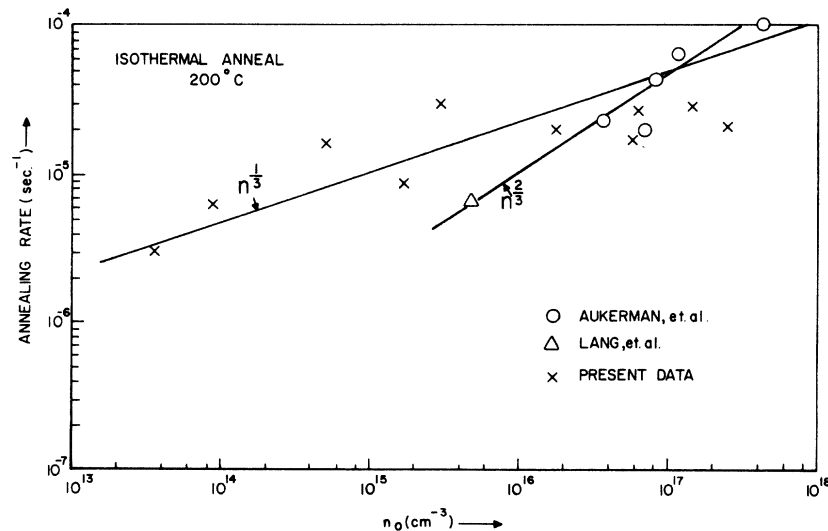


FIG. 6. Annealing rate vs  $n_0$  for the  $\lambda_2$  substage. The solid lines represent possible functional dependences of  $\lambda_2$  on  $n_0$ ; i.e.,  $\lambda_2 \propto n_0^{1/3}$  and  $\lambda_2 \propto n_0^{2/3}$ . See text for details.

or with imperfections already existing in the sample. In the case of GaAs, and indeed most semiconductors, it is generally assumed that interstitials are mobile below room temperature; therefore any stable defect which can interact with interstitials could be expected to have a nonlinear production rate. The fact that both the functional dependence and the absolute value of the production rate vary so widely from sample to sample makes quantitative calculations of defect production from the appropriate rate equations of questionable value. However, a brief qualitative discussion of a simple model of vacancy production in the presence of free interstitials is probably useful. The two relevant rate equations are

$$\frac{dn_i}{dt} = K \frac{d\phi}{dt} - (\sigma_s N_s + \sigma_v n_v) n_i v_i, \quad (2)$$

$$\frac{dn_v}{dt} = K \frac{d\phi}{dt} - \sigma_v n_v n_i v_i, \quad (3)$$

where  $n_i$  is the free-interstitial concentration,  $n_v$  is the vacancy concentration,  $K$  is the proportionality constant that gives the rate of vacancy-interstitial pair production,  $\sigma_s$  is the capture cross section of sinks for free interstitials,  $\sigma_v$  is the capture cross section of vacancies for free interstitials,  $v_i$  is the velocity of the free interstitials, and  $N_s$  is the concentration of interstitial sinks (excluding vacancies). The interstitial sinks in this model include traps, but re-emission from these traps is ignored. If it is assumed that free interstitial equilibrium is reached in a time which is short compared to the other relevant experimental times, then we can let  $dn_i/dt \approx 0$ , and from Eq. (2),

$$n_i = \frac{K d\phi/dt}{(\sigma_s N_s + \sigma_v n_v) v_i}. \quad (4)$$

In this approximation Eq. (3) yields

$$\frac{dn_v}{dt} = K \frac{d\phi}{dt} \left( \frac{\sigma_s N_s}{\sigma_s N_s + \sigma_v n_v} \right). \quad (5)$$

In the derivation of Eq. (5) one might justifiably object to the use of velocity (i.e.,  $v_i$ ), which is an ill-defined concept if the process is random walk in nature. However, Eq. (5) can be derived immediately by assuming that the created interstitials are "instantaneously" (on the time scale of  $K d\phi/dt$ ) either annihilated at the  $n_v$  or trapped at the  $N_s$ . Then the bracketed term in Eq. (5) is obviously the surviving fraction of the  $n_v$ .

In this simple model the production of  $n_v$  will be linear with fluence only if  $\sigma_v n_v \ll \sigma_s N_s$ . Such a situation cannot, of course, obtain for too long a time, because eventually the vacancy concentration will be high enough to compete with the sinks and traps for the mobile interstitials. Thus, if vacancies are important in the free-carrier removal process, and if interstitials are mobile at room temperature, the model

described here can account for some of the wide variation in carrier removal rates reported in the literature. It is, of course, not surprising that interstitial sinks and traps would vary in type and concentration with sample growth conditions. We also reiterate that flux dependences evidently do not account for the variation in the removal rates.

Another potentially important source of variation in the reported free-carrier removal rates is the position of the Fermi level, which will affect the proportionality between the defect introduction rate and the free-carrier removal rate. This effect is especially prominent in our purer samples ( $n_0 \leq 10^{15} \text{ cm}^{-3}$ ). At least seven defects are known to be introduced by electron irradiation<sup>12-15</sup>; however, because the Fermi level always lies within about 0.4 eV of the conduction band (at 200 °C or lower) in our samples, we need explicitly consider only those defects which lie above this value. Given a constant defect introduction rate, the free-carrier removal rate as a function of  $n_0$  can be calculated directly from the probability of occupation for each defect level. The curve in Fig. 3 is obtained by assuming that acceptors are introduced at 0.16 and 0.31 eV with introduction rates 2.2 and  $0.8 \text{ cm}^{-1}$ , respectively. (Electrical measurements in this work revealed levels at 0.15 and 0.31 eV; however, slightly better agreement is obtained assuming 0.16 instead of 0.15 eV.) The deviation of the data from the calculated curve at high doping levels is consistent with the observation of a shallow defect level at  $\sim 0.03 \text{ eV}$ .<sup>16</sup> However, the agreement of this curve with the data is by no means unique. Similar results can be obtained by assuming that one or both of the levels are donors if a deep acceptor is also introduced at a constant rate. It should be noted that while electrical measurements generally uncover only two defect levels in this region ( $\sim 0.15$  and  $\sim 0.30 \text{ eV}$ ), DLTS measurements routinely yield three levels (0.13, 0.20, and 0.31 eV). The data in Fig. 3 are not precise enough to preclude the presence of three levels in this region.

By using data from both production and annealing studies, it is possible to extract information concerning the production rate of defects in each substage ( $\lambda_1$  and  $\lambda_2$ ). The data in Tables I and II, for the  $\lambda_1$  and  $\lambda_2$  substages, respectively, were obtained in the following manner. The column labeled  $dn_T/d\phi$  in each table is simply the total free-carrier removal rate as determined from production data. The columns  $dn_1/d\phi$  (Table I) and  $dn_2/d\phi$  (Table II) are obtained from the fraction of free carriers which recover in each of the two annealing substages; i.e.,  $\Delta n_T = \Delta n_1 + \Delta n_2$ . By using the known energy levels of the defects near the conduction band (i.e., within 0.31 eV), the probability of electron occupation for each of them can be determined from the position of the Fermi level; thus, the introduction rates of the separate defects can be calculated.

TABLE I.  $\lambda_1$  substage defect production rates as a function of  $n_0$ .

Sample	$n_0$ ( $\text{cm}^{-3}$ )	$dn_T/d\phi$ ( $\text{cm}^{-1}$ ) <sup>a</sup>	$dn_1/d\phi$ ( $\text{cm}^{-1}$ ) <sup>b</sup>	$dE3^A/d\phi$ ( $\text{cm}^{-1}$ ) <sup>c</sup>	$dE3^D/d\phi$ ( $\text{cm}^{-1}$ ) <sup>d</sup>
TI-76B1-41A	$2.4 \times 10^{17}$	5.6	2.5	2.5	2.5
-26	$1.3 \times 10^{17}$	3.6	1.8	1.8	1.8
-89	$6.0 \times 10^{16}$	2.6	1.2	1.2	1.2
HP-C-7-3-5	$2.0 \times 10^{15}$	1.4 <sup>e</sup>	0.32 <sup>e</sup>	0.32	0.32
-6-1-39B	$5.0 \times 10^{14}$	0.83 <sup>e</sup>	0.39 <sup>e</sup>	0.40	0.39
-6-1-24	$2.0 \times 10^{14}$	0.16	0.03	0.22	0.05
-4-2-1	$1.5 \times 10^{14}$	0.35	0.05	0.56	0.11

<sup>a</sup>Total free-carrier removal rate.

<sup>b</sup>Free carriers removed by  $\lambda_1$  defects.

<sup>c</sup>Calculated introduction rate assuming that  $E3$  are acceptors.

<sup>d</sup>Calculated introduction rate assuming that  $E3$  are donors.

<sup>e</sup>Measurements were carried out at room temperature after successive 200 °C isothermal annealing steps; all other measurements were made *in situ* at 200 °C.

Capacitance studies in the literature give an identification of  $E1$  and  $E2$  with the  $\lambda_2$  substage, and  $E3$  with the  $\lambda_1$  substage.<sup>7</sup> In addition, for the case of  $\lambda_1$ , at least one other deeper level has also been identified as having the same annealing kinetics as  $E3$ ; i.e., the  $\lambda_1$  substage evidently involves more than just  $E3$ . In particular a hole trap,  $H1$ , near the valence band is sometimes introduced at a similar rate to  $E3$ .<sup>7</sup> For this reason, two cases are considered for the analysis of the introduction rate of  $E3$  from the production and annealing data. First,  $E3$  is assumed to be an acceptor, and second  $E3$  is assumed to be a donor while  $H1$  is an acceptor which is introduced at the same rate. The last two columns in Table I give the total introduction rate of  $E3$  under

these two assumptions. In both cases, the production rate of  $E3$  is seen to decrease significantly in the more pure samples. A third possibility is that  $E3$  is a donor introduced at a nearly constant rate, and that  $H1$  is produced at a decreasing rate in the purer samples. This point will be discussed later in more detail.

In Table II two cases are considered. First, it is assumed the  $\lambda_2$  arises solely from the 0.15-eV level,  $N_2$ , observed in this work; second, it is assumed that  $E1$  and  $E2$  are separate defects associated with  $\lambda_2$ . In this second case the relative introduction rates of  $E1$  and  $E2$  are taken from capacitance studies.<sup>12</sup> In both cases the introduction rate of the defects is nearly constant except for the purest samples. If no other defects are involved with the  $\lambda_2$  substage, then

TABLE II.  $\lambda_2$  substage defect production rates as a function of  $n_0$ .

Sample	$n_0$ ( $\text{cm}^{-3}$ )	$dn_T/d\phi$ ( $\text{cm}^{-1}$ ) <sup>a</sup>	$dn_2/d\phi$ ( $\text{cm}^{-1}$ ) <sup>b</sup>	$dN_2^A/d\phi$ ( $\text{cm}^{-1}$ ) <sup>c</sup>	$d(E1 + E2)^A/d\phi$ ( $\text{cm}^{-1}$ ) <sup>d</sup>
TI-76B1-41A	$2.4 \times 10^{17}$	5.6	3.1	4.1	3.7
-26	$1.3 \times 10^{17}$	3.6	1.8	3.0	2.5
-89	$6.0 \times 10^{16}$	2.6	1.4	3.4	2.5
HP-C-7-3-5	$2.0 \times 10^{15}$	1.4 <sup>e</sup>	1.1 <sup>e</sup>	4.0	2.1
-6-1-39B	$5.0 \times 10^{14}$	0.83 <sup>e</sup>	0.61 <sup>e</sup>	7.1	2.4
-6-1-24	$2.0 \times 10^{14}$	0.16	0.13	57	22
-4-2-1	$1.5 \times 10^{14}$	0.35	0.30	170	75

<sup>a</sup>Total free-carrier removal rate.

<sup>b</sup>Free-carriers removed by  $\lambda_2$  defects as determined from annealing data (see text).

<sup>c</sup>Calculated introduction rate, assuming a single acceptor at 0.15 eV.

<sup>d</sup>Calculated introduction rate assuming two acceptors ( $E1$  and  $E2$ ) at 0.13 and 0.2 eV, respectively.

<sup>e</sup>Measurements were carried out at room temperature after successive 200 °C isothermal annealing steps; all other measurements were made *in situ* at 200 °C.

the production of defects (both cases) grows very rapidly in the purest samples. Alternatively, it is possible that another deeper defect is annealing with similar kinetics. The latter explanation seems more likely. That is, a small concentration of a deep acceptor which varies randomly from sample to sample (accounting for  $\sim 0.3 \text{ cm}^{-1}$  removal rate in HP-C-4-2-1, for example) could account for the apparent large increase in  $N_2$  (or  $E1$  and  $E2$ ). The so-called  $H0$  level could be a candidate for this effect.

### B. Annealing

The electrical activity after a room-temperature irradiation is thought to result mainly from Ga-sublattice damage,<sup>2</sup> evidently because As-sublattice damage anneals at lower temperatures.<sup>9</sup> In many semiconductors interstitials move quite freely at room temperature, but there is some evidence that the Ga vacancy ( $V_{\text{Ga}}$ ) is stable, at least at temperatures below the 200 °C annealing stage.<sup>2</sup> In this case we would identify  $n_V$  with  $V_{\text{Ga}}$ , and  $n_i$  with  $\text{Ga}_i$ , in terms of the model presented earlier [Eqs. (2) and (3)]. Since it has been suggested that  $E3 \equiv V_{\text{Ga}}$ ,<sup>2</sup> and since  $E3$  anneals with  $\lambda_1$  kinetics,<sup>7,17</sup> the mechanism of vacancy motion must be considered in more detail. Also, the results discussed below, with trivial changes, can be applied to almost any thermally activated defect motion.

Vacancy motion is generally described in terms of the diffusion equation, which contains a single parameter  $D$ , the diffusion constant. The GaAs zincblende lattice is composed of Ga and As fcc sublattices, respectively, and for diffusion on such a sublattice  $D$  is given by

$$D = a_0^2 \nu = a_0^2 \nu_0 \exp(\Delta S_m/k) \exp(-\Delta H_m/kT) \quad (6)$$

where  $a_0/\sqrt{2}$  and  $\nu$  are the elemental jump distance and frequency, respectively,  $\nu_0$  is an "attempt-to-escape" frequency, and  $\Delta S_m$  and  $\Delta H_m$  are the entropy and enthalpy of motion, respectively. For GaAs,  $a_0 \approx 5.64 \text{ \AA}$ , and we may estimate  $\nu_0$  from the Debye temperature; i.e.,  $\nu_0 = k \theta_D/h \approx 7 \times 10^{12} \text{ sec}^{-1}$ . Studies of  $\Delta S_m$  in the III-V compounds are scarce, but in the alkali halides<sup>18</sup>  $\Delta S_m/k \approx 1-3$ , and in Si and Ge,<sup>19</sup>  $\Delta S_m/k \approx 4$ . Thus, in order of magnitude, it is not unreasonable to estimate  $\exp(\Delta S_m/k) \approx 10$ , which then gives  $D \approx 10^{-1} \exp(-\Delta H_m/kT)$ . It is interesting to compare this result with that of Chiang and Pearson<sup>20</sup> who found  $D(V_{\text{Ga}}) \approx 2 \times 10^{-3} \times \exp(-2.1/kT)$ , over the range 700–1000 °C. If this latter value can be extrapolated to 200 °C, then it would suggest that  $\nu(V_{\text{Ga}}) \approx 6 \times 10^{11} \times \exp(-2.1/kT)$  in our annealing region. This point will be discussed further later.

So far we have considered only elemental jumps,

for which the jump rate, from Eq. (6), is  $\nu_0 \exp(\Delta S_m/k) \exp(-\Delta H_m/kT)$ . In an annealing process, however, the moving species may have to make, say  $N_j$  jumps, on the average, before the annihilation event. Thus, the rate relevant to annealing processes will be given by

$$\lambda = \frac{\nu_0}{N_j} \exp(\Delta S_m/k) \exp(-\Delta H_m/kT) \quad (7)$$

As mentioned earlier, in relatively doped samples ( $n_0 \geq 10^{16} \text{ cm}^{-3}$ ), we find two annealing stages near 200 °C, with

$$\lambda_1 = 3 \times 10^8 \exp(-1.2/kT) \quad (8a)$$

$$\lambda_2 = 1 \times 10^{12} \exp(-1.6/kT) \quad (8b)$$

By carefully extracting data from plots given by Aukerman and Graft,<sup>1</sup> and by Lang *et al.*<sup>7,19</sup> we find quite similar results. Furthermore, all workers conclude that both annealing stages are first-order [as defined by Eq. (1)] to within experimental accuracies, and that  $\lambda_1$  is independent of  $n_0$ . The situation for  $\lambda_2$  is somewhat different, as shown in Fig. 6. Aukerman and Graft<sup>1</sup> find that  $\lambda_2 \propto n_0$ , with much scatter in their data. When Lang<sup>7</sup> adds his point to those of Aukerman and Graft he suggests that  $\lambda_2 \propto n_0^{2/3}$ . (Note that these authors are dealing with rather impure samples, i.e.,  $n_0 \geq 10^{16} \text{ cm}^{-3}$ ). Our points alone, on the other hand, would be consistent with  $\lambda_2$  independent of  $n_0$ , at least for  $n_0 \geq 10^{15} \text{ cm}^{-3}$ . By including everybody's points, the best fit is perhaps  $\lambda_2 \propto n_0^{1/3}$ . All of these relationships may be obtained theoretically. For example, if  $R$  is the average distance between impurities, and if the annealing process involves movement to an impurity, then a *direct* movement would give  $N_j \approx R/a_0$ , or  $\lambda_2 \propto n_0^{1/3}$ , whereas a diffusive (random-walk) movement would give  $N_j \approx R^2/a_0^2$ , or  $\lambda_2 \propto n_0^{2/3}$ . If, however, the annealing process were independent of the impurity concentration, then  $\lambda_2$  would be independent of  $n_0$ , of course. Finally, a charge-state dependent mechanism<sup>1</sup> yields  $\lambda_2 \propto n_0$ . The scatter in the data would seem to preclude a definite determination of the relationship between  $\lambda_2$  and  $n_0$ , although in our data it does appear that  $\lambda_2$  diminishes for  $n_0 < 10^{15} \text{ cm}^{-3}$ . Even this latter conclusion is subject to some uncertainty because of the increased measurement difficulties in these very pure samples. That is, the resistivities are stronger functions of temperature, making more precise temperature control necessary. This problem is compounded by the necessarily larger data accumulation times caused by the smaller annealing rates.

Two other observations concerning the annealing should be pointed out. One is that the *fraction* of  $\lambda_2$  defects, i.e.,  $\Delta n_2/\Delta n_1$  as defined in Eq. (1), appears to increase in the purer samples. The other observation is that in the very pure samples *reverse* annealing

is sometimes seen in the  $\lambda_1$  substage. These points will be discussed later.

To explain first-order annealing we must consider the following possible mechanisms: (i) Frenkel-pair annihilation for which we would normally expect a prefactor  $\nu_p \equiv \nu_0 N_j^{-1} \exp(\Delta S_m/k) \approx 10^{13} \text{ sec}^{-1}$ ; (ii) long-range migration to an "infinite" sink, for which we would expect  $\nu_p \ll 10^{13} \text{ sec}^{-1}$ , with  $\nu_p$  dependent upon the sink concentration; and (iii) the breakup of a complex, for which the observed activation energy is now a *dissociation* energy, rather than a motional energy. Mechanism (iii) could itself involve two different processes: (a) the breakup of an irradiation-induced defect; or (b) the breakup of a pre-existing complex which then releases a species capable of finding and annihilating the irradiation-induced defect. For mechanism (b) the moving species must be of semi-infinite concentration in order to give first-order kinetics. For both mechanisms (a) and (b),  $\nu_p \approx 10^{13} \text{ sec}^{-1}$ , unless there is retrapping involved, in which case we can have  $\nu_p \ll 10^{13} \text{ sec}^{-1}$ .

We now compare the existing annealing data with these possible mechanisms. It first must be noted that according to the DLTS results there are at least three defects (*E3*, *E5*, and *H1*) associated with the  $\lambda_1$  annealing stage, and two defects (*E1* and *E2*) associated with  $\lambda_2$ .<sup>2,7</sup> Each of these defects is seen only in irradiated samples. Lang *et al.*<sup>2</sup> have presented a model in which *E3* is an isolated Ga vacancy, and *E1* and *E2* are also isolated native defects associated with the Ga sublattice, such as  $\text{Ga}_i$  or  $\text{As}_{\text{Ga}}$ . The *E5* and *H1* production rates vary from sample to sample and thus these defects are evidently complexes.

To account for three defects (*E3*, *E5*, and *H1*) annealing with the same kinetics ( $\lambda_1$ ) is very difficult unless we invoke mechanism (b). For if only one of them moves (say *E3*) how does it exactly annihilate the other two, especially with first-order kinetics? And it is certainly unlikely that all three either move or break up equally well at a given temperature. It seems more likely that a completely different species moves and annihilates all three defects.

Let us consider a simple version of how this might happen. Suppose that as a result of its growth process a crystal contains a concentration  $N_t$  of a particular center which is capable of trapping some relatively mobile species, say  $\text{Ga}_i$ . The  $N_t$  may be impurities or dislocations of some type. Further suppose that the irradiation induces some defect, say  $V_{\text{Ga}}$ , which can be annihilated by the mobile species. Then, in analogy with Eq. (5), the appropriate rate equation would be

$$\frac{dn_d}{dt} = -\nu n_{mt} \frac{n_d \sigma_d}{N_t \sigma_t + n_d \sigma_d}, \quad (9)$$

where  $n_d$  is the concentration of the radiation-induced defect,  $n_{mt}$  is the concentration of the mobile species trapped at a given time, and  $\nu$  is the release

(detrapping) rate. Equation (9) is valid if a released  $n_m$  is *immediately* either recaptured at an  $N_t$  or annihilated at an  $n_d$ . That is, in this model, the rate of the process must not be limited by the *motion* of the  $n_m$  but only by their detrapping frequency. If  $n_d \sigma_d \ll N_t \sigma_t$ , and if the irradiation process itself adds at most only a small percentage to the  $n_{mt}$  (or, roughly requiring  $n_d \ll n_{mt}$ ), then Eq. (9) describes a first-order process with an effective frequency factor,  $\nu_{\text{eff}}$ , given by

$$\frac{dn_d}{dt} = -\nu n_{mt} \frac{n_d \sigma_d}{N_t \sigma_t} = -n_d \frac{\nu n_{mt} \sigma_d}{N_t \sigma_t} \equiv -n_d \nu_{\text{eff}}. \quad (10)$$

To be able to use a constant  $N_t$  in the denominator of  $\nu_{\text{eff}}$  we are implicitly assuming either that  $n_{mt} \ll N_t$ , or that each  $N_t$  can absorb more than one of the  $n_m$  with equal probability.

If during the cooling phase of the growth process the  $N_t$  traps had competition from other traps and sinks for capture of the  $n_m$ , then we might expect that  $n_{mt} \propto N_t$ , or  $n_{mt} = AN_t$ , giving

$$\nu_{\text{eff}} \approx \frac{\nu_0 A \sigma_d}{\sigma_t} \exp(-E_r/kT), \quad (11)$$

where  $\nu_0 \exp(-E_r/kT)$  is the release rate of the  $n_m$ . The annihilation process described by Eq. (11) is first order, independent of trap concentration and has a prefactor different from  $\nu_0$  by the factor  $A \sigma_d / \sigma_t$ . These characteristics are all observed in the  $\lambda_1$  annealing process, for which we would then identify  $E_r \approx 1.2 \text{ eV}$  and  $A \sigma_d / \sigma_t \approx 10^{-4}$ . However, a further complication arises in that the  $\lambda_1$  substage involves more than one defect, and thus more than one  $\sigma_d$ . That is, for *E3*, *E5*, and *H1* all to anneal at just one rate ( $\lambda_1$ ), their respective  $\sigma_d$ 's must not be too different, according to Eq. (11). This situation could obtain if *E3*, *E5*, and *H1* were all  $V_{\text{Ga}}$  related, and if the  $n_m$  were  $\text{Ga}_i$ ; however, if the  $V_{\text{Ga}}$  are immobile at room temperature then how would the *E5* and *H1* complexes ever be initially formed? Two possibilities exist: (i) recombination-enhanced motion<sup>21</sup> of the  $V_{\text{Ga}}$ , under the influence of the electron beam; and (ii) recombination-enhanced motion of certain impurities, which can then interact with the  $V_{\text{Ga}}$ . These ideas are quite speculative and will not be pursued further.

One interesting feature of the above model is that it does not require *E3* to move during the 200 °C annealing process. If *E3* is the Ga vacancy, then its lack of motion would be consistent with the results of Chiang and Pearson (CP)<sup>20</sup> who found that  $D(V_{\text{Ga}}) \approx 2 \times 10^{-3} \exp(-2.1/kT)$  in the range 700–1000 °C. That is, if the CP result can be extrapolated to 200 °C, then *elementary* vacancy jumps should occur at a rate  $\nu \approx D/a_0^2 \approx 3 \times 10^{-11} \text{ sec}^{-1}$ , much too slow to account for our observed annihilation rate,  $\lambda_1(200 \text{ °C}) \approx 5 \times 10^{-5} \text{ sec}^{-1}$ .

To conclude the  $\lambda_1$  discussion it may be noted that the model presented here is quite complex, at least compared to the alternative that  $E3$  moves at 200 °C and undergoes long-range migration to annihilate  $E5$  and  $H1$ . But this latter model seems to be inconsistent with the first-order kinetics and sample independence of  $\lambda_1$ . Furthermore, if  $E3 \equiv V_{Ga}$ , then there is also an inconsistency with the CP result, although this is a less serious problem because of the necessary temperature extrapolation to compare results.

Lang *et al.*<sup>2</sup> have also suggested that  $E1$  and  $E2$  ( $\lambda_2$  substage) are isolated native defects and may, in fact be two charge states of the same defect. If Frenkel pairs can be dismissed, then the two most likely candidates for such a defect would be the antisite defects,  $As_{Ga}$  and  $Ga_{As}$ . (Note that the  $Ga_i$  are expected to be mobile, and there is already some evidence that  $V_{Ga} \equiv E3$ , as discussed earlier.) The  $As_{Ga}$  and  $Ga_{As}$  defects would naively be expected to be double donors and acceptors, respectively. The latter seems a much more probable candidate for  $E1$  and  $E2$  since it would remove carriers during production and return them during the anneal, as observed. The  $As_{Ga}$  candidate on the other hand, would require a "matching" acceptor to anneal at the same time, and the existence of such an additional defect has not yet been confirmed. The formation of antisite defects could presumably occur either by knock-on events or by migration of one of the partners, probably the interstitial. (If the migration were long range then the production might be supralinear.)

The  $\lambda_2$  annealing process has first-order kinetics and a relatively high prefactor. These attributes again suggest a breakup process, say  $Ga_{As} \rightarrow Ga_i + V_{As}$ , where the observed activation energy (1.6 eV) would be a dissociation energy. If both of the dissociation products, i.e.,  $Ga_i$  and  $V_{As}$ , had high mobility at 200 °C, they would quickly find sinks or traps and thus would not affect the  $\lambda_2$  annealing rate, even if they or their subsequent complexes were electrically active. (Any electrical activity, of course, could affect  $\Delta n_2$ .) If, however, the trapping times of the free  $Ga_i$  and/or  $V_{As}$  were not totally negligible compared to the average dissociation time of the  $Ga_{As}$ , then the effective  $\lambda_2$  could be lower in the purer samples, as observed. Any significant reassociation of the  $Ga_i$  and  $V_{As}$ , i.e.,  $Ga_i + V_{As} \rightarrow Ga_{As}$ , would again lower the prefactor of  $\lambda_2$ , and this process would also be more prevalent in the purer samples; however, it could affect the order of the kinetics. Further discussion of  $\lambda_2$  does not seem warranted since the actual dependence of  $\lambda_2$  upon  $n_0$  is ambiguous anyway.

The above models for the various defects permit a natural interpretation of why the ratio  $\Delta n_1/\Delta n_2$  decreases with decreasing impurity concentration. That is, if  $H1$  is an acceptor lying well below midgap then it will always contribute effectively to the  $\Delta n_1$  carrier

removal in *n*-type samples. However, according to the DLTS results, the production rate of  $H1$  varies with sample purity,<sup>2</sup> and thus we see that the higher-purity samples may contain a lower fraction of  $\Delta n_1$ . In fact, we often observe a *reverse* annealing effect in very high-purity samples. That is, at the beginning of the anneal the electron concentration actually *decreases* for a time ( $\sim 1/\lambda_1$ ) before the  $\lambda_2$  process begins to take over. This effect could be well explained if  $E3$  were a *donor* because then, in the absence of  $H1$ , the  $\lambda_1$  annealing process would *remove* instead of *add* electrons. In the more impure samples  $E3$ , as a donor, would lie well below the Fermi level and thus not affect either the production or the annealing. This discussion of the reverse annealing phenomenon must be regarded as tentative, however, since measurement problems have not been eliminated as a possible cause.

Thus, the model best fitting our data, we believe, includes  $E3$  as a donor,  $H1$  as an acceptor, and  $E1$  and  $E2$  also as acceptors, or perhaps the two charge states of a double acceptor. Two other defects seen by DLTS,  $E4$  and  $E5$ , are probably not important to the above discussion since their production rates are evidently quite low.<sup>7</sup> Another defect,  $H0$ , has been seen both by electrical measurements<sup>13,14,22</sup> and DLTS,<sup>7</sup> but little is known of its production rate. However, the rate may well be high since it is possible, in some *n*-type samples, to drive the Fermi level down nearly to the  $H0$  level.<sup>22</sup> If  $H0$  happens to anneal with either  $\lambda_1$  and  $\lambda_2$  kinetics, then the model presented above would be materially affected.

One disturbing feature of this model is the assignment of  $E3$  as a donor, which seems to be in conflict with the evidence that  $E3$  is the Ga vacancy. That is, we would naively expect the Ga vacancy to be an acceptor, not a donor. Another candidate for  $E3$  might be  $As_{Ga}$ , but independent evidence for this assignment is lacking. In short, there are still many questions to be resolved before a totally acceptable model can be established.

## V. SUMMARY

Our study of the production and annealing of electron-irradiated GaAs has led to the following conclusions:

(i) Room-temperature defect production is nearly always sublinear with fluence. This can be explained by a simple model of stable (or nearly stable) Ga vacancies competing with traps and sinks for the mobile Ga interstitials.

(ii) The wide variation in reported free-carrier removal rates cannot be accounted for by a flux dependence. Some of the variation is probably due to the formation of defect-impurity complexes, which may include  $E5$  and  $H1$ . Another factor, quite important

in high-purity samples, is the position of the Fermi level, which can change the proportionality between the *defect-production* rate and the *carrier-removal* rate.

(iii) The 200 °C annealing stage includes two first-order substages with annealing rates close to those reported in the literature. Besides being first order, the first substage ( $\lambda_1$ ) also is nearly independent of sample growth conditions and doping levels and has a relatively low prefactor. These attributes can be explained by a model in which the  $\lambda_1$  substage involves Ga-vacancy related defects annealing by interactions with Ga interstitials which are themselves emitted by interstitial traps. The  $\lambda_2$  substage is also best described by a dissociation process, perhaps involving Ga<sub>As</sub>. The rate  $\lambda_2$  appears to decrease with decreasing  $n_0$  although the exact relationship is not clear.

(iv) The defect model most consistent with all of the data includes *E3* as a donor, *H1* as an acceptor, and *E1* and *E2* as the two charge states of a double acceptor. The exact identifications of these defects are, however, somewhat in doubt and must await further experimentation.

#### ACKNOWLEDGMENTS

We wish to thank Gary McCoy for growing many of the VPE GaAs samples used in this study, and Donald Locker for many helpful discussions regarding the experimental aspects of the work. Work performed at the Avionics Laboratory, Wright-Patterson AFB, under Contract No. F33615-76-C-1207.

- 
- <sup>1</sup>L. W. Aukerman and R. D. Graft, *Phys. Rev.* **127**, 1576 (1962).
- <sup>2</sup>D. V. Lang, R. A. Logan, and L. C. Kimerling, *Phys. Rev. B* **15**, 4874 (1977).
- <sup>3</sup>E. H. Putley, *The Hall Effect and Semiconductor Physics*. (Dover, New York, 1968), Chap. 2.
- <sup>4</sup>T. I. Kol'chenko and V. M. Lomako, *Sov. Phys. Semicond.* **9**, 1157 (1975).
- <sup>5</sup>J. A. Moore, G. Carter, and A. W. Tinsley, *Radiat. Eff.* **25**, 49 (1975).
- <sup>6</sup>Wayne J. Anderson and Y. S. Park, *J. Appl. Phys.* **49**, 4568 (1978).
- <sup>7</sup>D. V. Lang, in *Conference on Radiation Effects in Semiconductors, Dubrovnik, Yugoslavia, 1976*, edited by N. B. Uri and J. W. Corbett, IOP Conf. Proc. No. 31 (Institute of Physics, London, 1977), p. 70.
- <sup>8</sup>P. L. Pegler, J. A. Grimshaw, and P. C. Banbury, *Radiat. Eff.* **15**, 183 (1972).
- <sup>9</sup>K. Thommen, *Radiat. Eff.* **2**, 201 (1970).
- <sup>10</sup>A. Kahan, L. Bouthillette, and H. M. DeAngelis, *Radiat. Eff.* **2**, 99 (1971).
- <sup>11</sup>A. H. Kalma and R. A. Berger, *IEEE Trans. Nucl. Sci.* **19**, 209 (1972).
- <sup>12</sup>D. V. Lang and L. C. Kimerling, in *Conference on Lattice Defects in Semiconductors, Freiburg, 1974*, edited by F. A. Huntley, IOP Conf. Proc. No. 23 (Institute of Physics, London, 1975), p. 581.
- <sup>13</sup>N. A. Vitovskii, T. V. Mashovets, S. M. Ryvkin, and R. Yu. Khanevarov, *Sov. Phys. Solid State* **5**, 2575 (1964).
- <sup>14</sup>G. E. Brehm and G. L. Pearson, *J. Appl. Phys.* **43**, 568 (1974).
- <sup>15</sup>J. K. O'Brien and J. C. Corelli, *J. Appl. Phys.* **44**, 1921 (1973).
- <sup>16</sup>T. I. Kol'chenko and V. M. Lomako, *Radiat. Eff.* **37**, 67 (1978).
- <sup>17</sup>L. C. Kimerling and D. V. Lang, in *Conference on Lattice Defects in Semiconductors, Freiburg, 1974*, edited by H. A. Huntley, IOP Conf. Proc. No. 23 (Institute of Physics, London, 1975), p. 589.
- <sup>18</sup>P. Varotsos and K. Alexopoulos, *Phys. Rev. B* **15**, 2348 (1977).
- <sup>19</sup>J. A. Van Vechten, *J. Electrochem. Soc.* **122**, 423 (1975).
- <sup>20</sup>S. Y. Chiang and G. L. Pearson, *J. Appl. Phys.* **46**, 2986 (1975).
- <sup>21</sup>D. V. Lang, L. C. Kimerling, and S. Y. Leung, *J. Appl. Phys.* **47**, 3587 (1976).
- <sup>22</sup>J. W. Farmer and D. C. Look, *J. Appl. Phys.* **50**, 2970 (1979).